

Chapter 3

Experimental Methods

The major focus of the present study is to reconstruct high resolution monsoon records from $\delta^{18}O$ of speleothem samples distributed across the peninsular India and compare them with available terrestrial and oceanic records for possible coherence. The work also includes analysis of planktonic foraminifera from Andaman Sea.

The following chapter describes the detailed procedures for stable isotope and trace element measurements on five stalagmite samples collected from peninsular India. The chapter is divided into six sections. Section 3.1 describes samples collected and sub-sampling. In section 3.2, analysis of stable isotope ratios of carbon and oxygen in carbonates, and trace element measurements are discussed. Section 3.3 describes the meteorological data used in the present study. Focus of sections 3.4 and 3.5 is on ^{14}C geochronology and the U/Th dating technique used to date speleothems. Section 3.6 describes the sampling and analysis of a sediment core from the Andaman Sea.

3.1 Samples

A total of five stalagmites were collected and analyzed in the present study. All were cut along their growth axes using a Dramet cutting machine (Figure 3.1)

into four slices. One slice was used for stable isotope analysis, the second slice was used for the trace element studies, the third for U-Th dating and the fourth was archived. Sub-samples for stable isotopes were extracted using a New



Figure 3.1: *Dramet cutting machine at PRL used to slice speleothems.*

Wave Research Micro Mill with the maximum possible resolution of $\sim 200 \mu\text{m}$ (Figure 3.2). The system has a video microscope coupled to a high speed drill and a set of computer controlled motorized stages. It uses a carborundum or diamond drill bit of $\sim 100 \mu\text{m}$ diameter. The sub-samples milled are stored in autoclavable polypropylene 0.2 ml tubes. The stable isotope measurements of the samples were carried out on Delta-V plus and MAT-253 Isotope Ratio Mass Spectrometers (IRMS) at the Physical Research Laboratory, Ahmedabad, India. The details of samples are discussed below.

The Dandak cave Two stalagmite samples were retrieved from the Dandak cave. Active calcium carbonate precipitation was seen on one of the samples

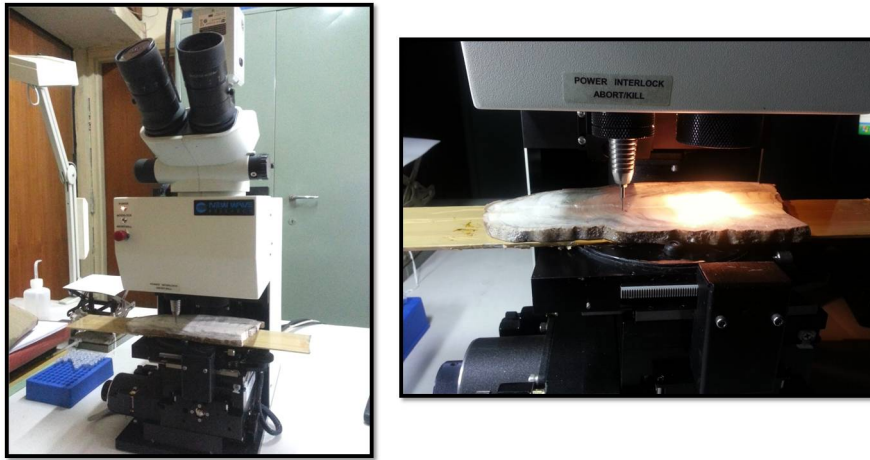


Figure 3.2: *Left: New Wave Research Micro Mill at PRL. Right: Sub-sampling of a stalagmite.*

referred to as Dan-I stalagmite. The tip of the stalagmite represents the year of its collection i.e. CE 1996. Length of the sample is ~ 29 cm and 1590 sub-samples were extracted for stable isotope measurements. The sample has a hiatus, which is seen as a discontinuity at the bottom. As shown in the figure 3.3, the layers below the hiatus are rich in detritus. The younger layers above the hiatus are made of white calcite crystals seen clearly in the thin section. The younger layers however are interrupted by thin laminations of detritus. The second stalagmite (Dan-II) has a length of 41.3 cm (Figure 3.4) and 2250 sub-samples were extracted for stable isotope analysis. The layers are made of pure calcite and show uninterrupted growth. The sample shows younger growth layers on the left side, in response to the re-activation of the drip water and shift in the drip site. Both the samples were sent to University of New Mexico, Mexico for U-Th geochronology.

The Kotumsar stalagmite The Kotumsar stalagmite (KOT-I) sample is a 29.6 cm long stalagmite (Figure 3.5), composed mostly of white calcite with its outer surface covered by gray calcitic layer (based on X-ray diffraction analyses). The sample, when cut open along its growth axis, can be divided into four bands

(I to IV, Figure 3.5) based on color and texture. All the bands show annual layers (1 mm thick in bands I, II and IV and 0.3 mm in band III) that can be viewed with the naked eye. In band III, distinct brown laminae, due to incorporation of soil impurities, are observed. High resolution sampling (Figure 3.6) was done using a micro-mill, with the spatial resolution of 200 μm ($\sim 3 - 5$ samples in a layer). Around 1277 subsamples were extracted weighing ~ 500 micro grams. Sub-samples for Hendy's test [Hendy, 1971] were extracted from four layers are shown in figure 3.6.

The Kailash cave The Kailash cave stalagmite with a length of 49 cm is the longest studied sample in the present study (Figure 3.7). The sample shows uninterrupted calcite growth layers. The thickness of the layers varies between $\sim 1 - 2$ mm and can be counted with the aid of hand-held lens. Total 146 layers were counted and 2872 subsamples were extracted for stable isotope measurements. The layers which are annual in nature have merged at some places to form thick white bands, making the counting difficult. The change in the growth axes at three different locations, point to a lateral shift of the drip site. The sample was sent to Taiwan University, Taiwan for geochronology.

The Belum cave The BLM-1 stalagmite was recovered from the inner gallery of cave having 100% humidity with a narrow channel to access. It is 31.4 cm long and shows distinct growth layers. The sample has three distinct growth zones representing the influence of different climatic regimes. The lower most section has white calcitic layers. The middle sections has high detritus with porous radial crystals and the uppermost has prominent growth layers. These three sections are separated by two hiatuses, one between the lower and the middle and other between the middle and the uppermost sections (Figure 3.8) respectively.



Figure 3.3: *Polished cross sectional view of the Dandak-I stalagmite. Planar view of the growth layers indicated constant shift in the drip direction, changing the growth axes. Near the bottom, a hiatus (Blue arrow) is observed as a distinct boundary separating two growth phases. Post hiatus, the growth axis has shifted and there is a continuous growth thereafter.*

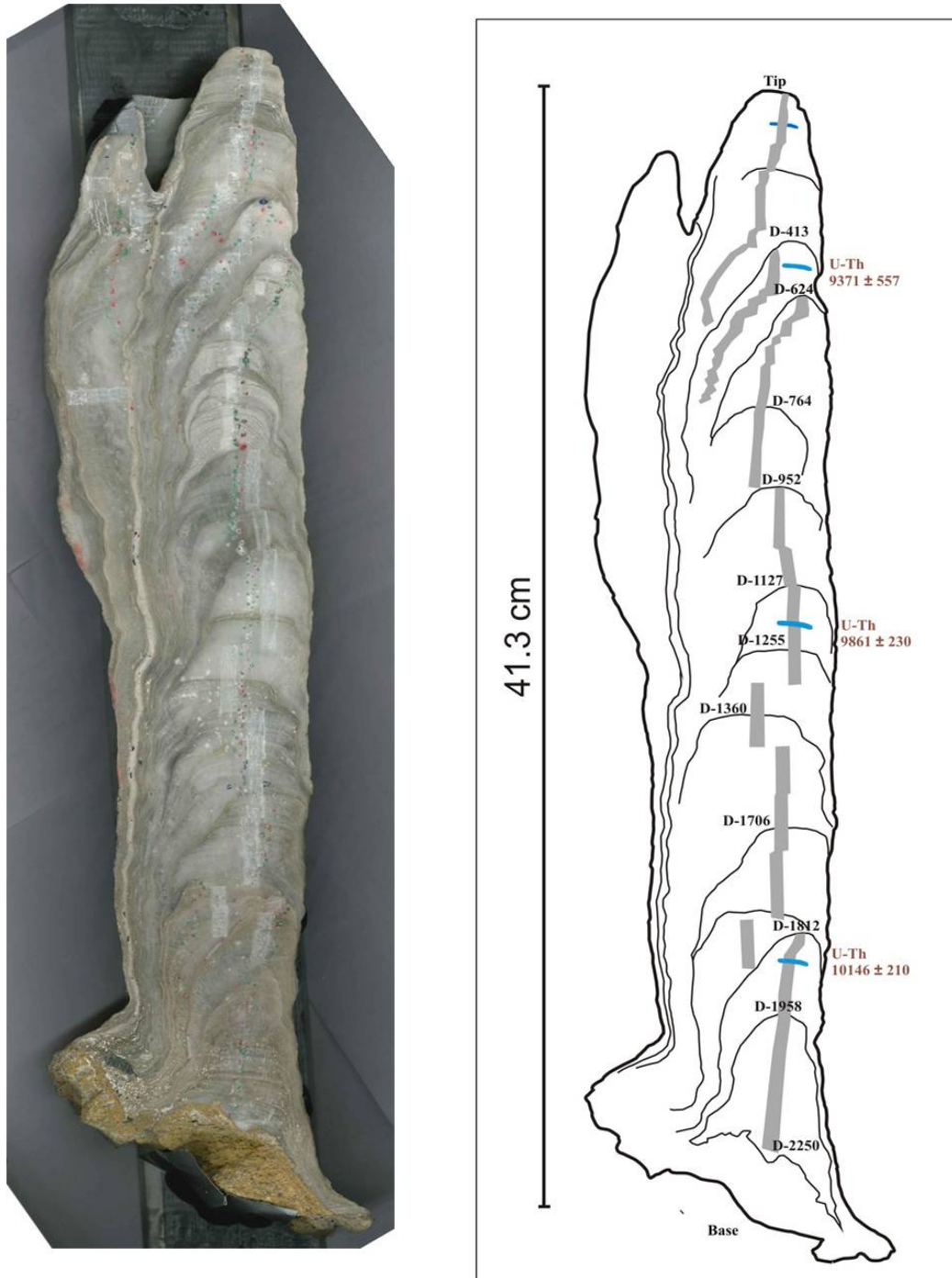


Figure 3.4: *Left: Polished cross sectional view of the Dandak-II stalagmite; .Right: Schematic cross section of Dandak-II stalagmite The gray bands represent high resolution sampling points for stable isotope analyses. Since the sampling resolution is $\sim 200 \mu\text{m}$, the band is seen as continuous. Four ^{230}Th dating points are marked by the blue lines.*

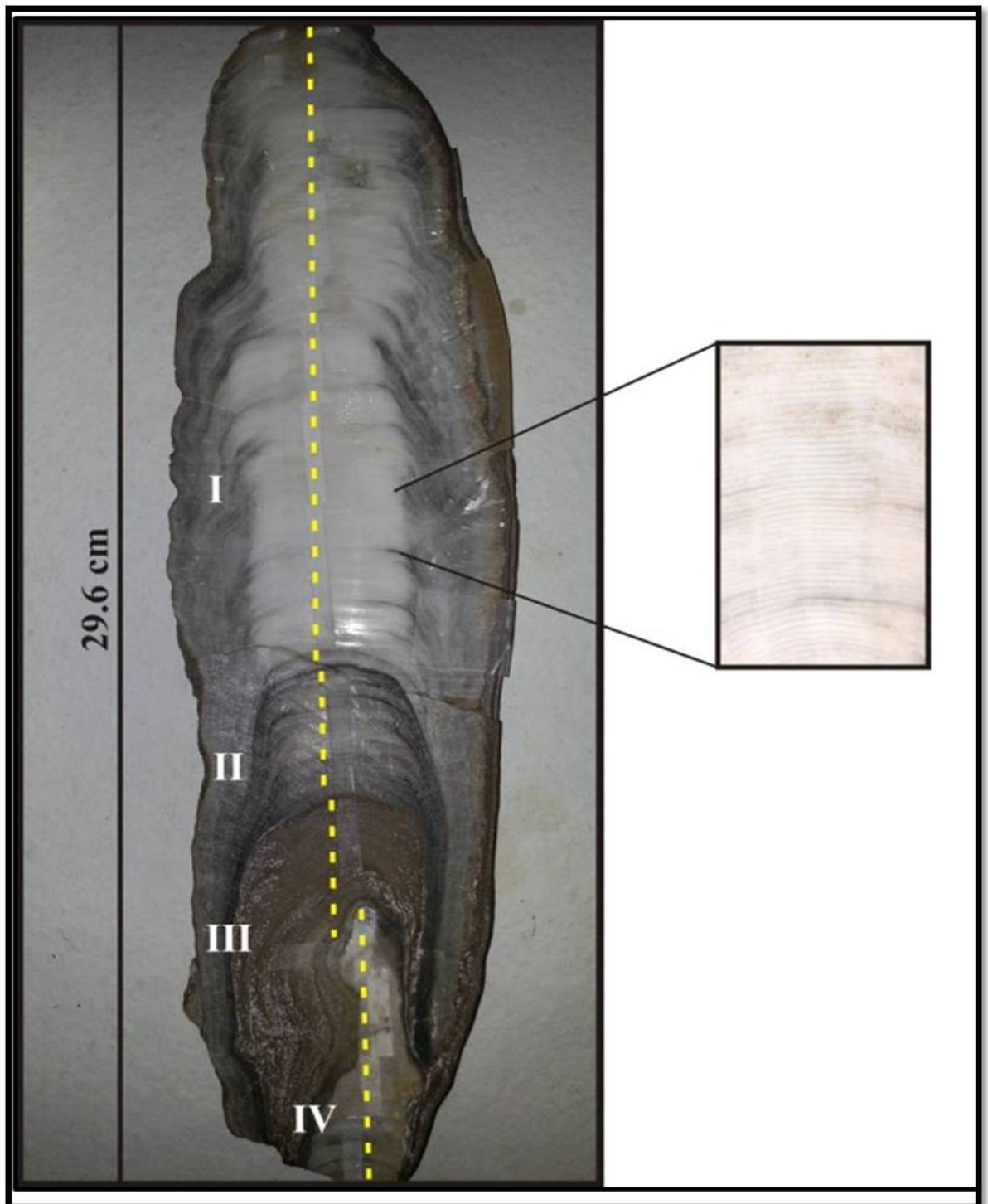


Figure 3.5: *Left: Polished cross sectional view of the KOT-I speleothem showing color bands; Right: Enlarged photo of part of the sample showing distinct layers that could be annual.*

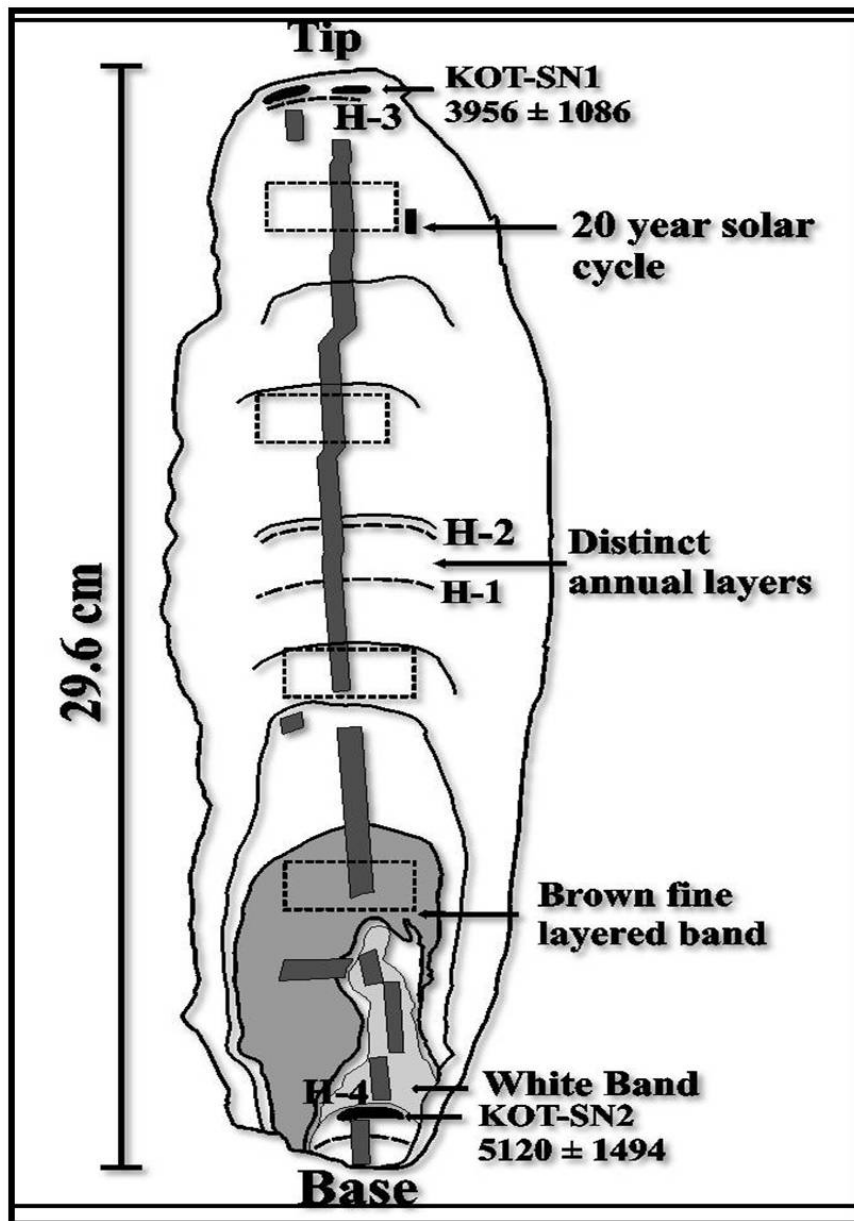


Figure 3.6: Schematic cross section of KOT-I. The dark lines indicate distinct layers that can be seen with the naked eye. Subsamples for the Hendy's test were extracted along dashed lines marked as H-1 to H-4. The dark vertical band in the middle, stretching from top to bottom, represents high resolution sampling points for stable isotope analyses. Since the sampling resolution is $\sim 200 \mu\text{m}$, the band is seen as continuous. Two ^{230}Th dates at the bottom and top are 5100 ± 1500 (SN-2) and 4000 ± 1100 (SN-1) years (errors at 2σ level), respectively. ^{14}C dating positions are shown as dashed rectangles.

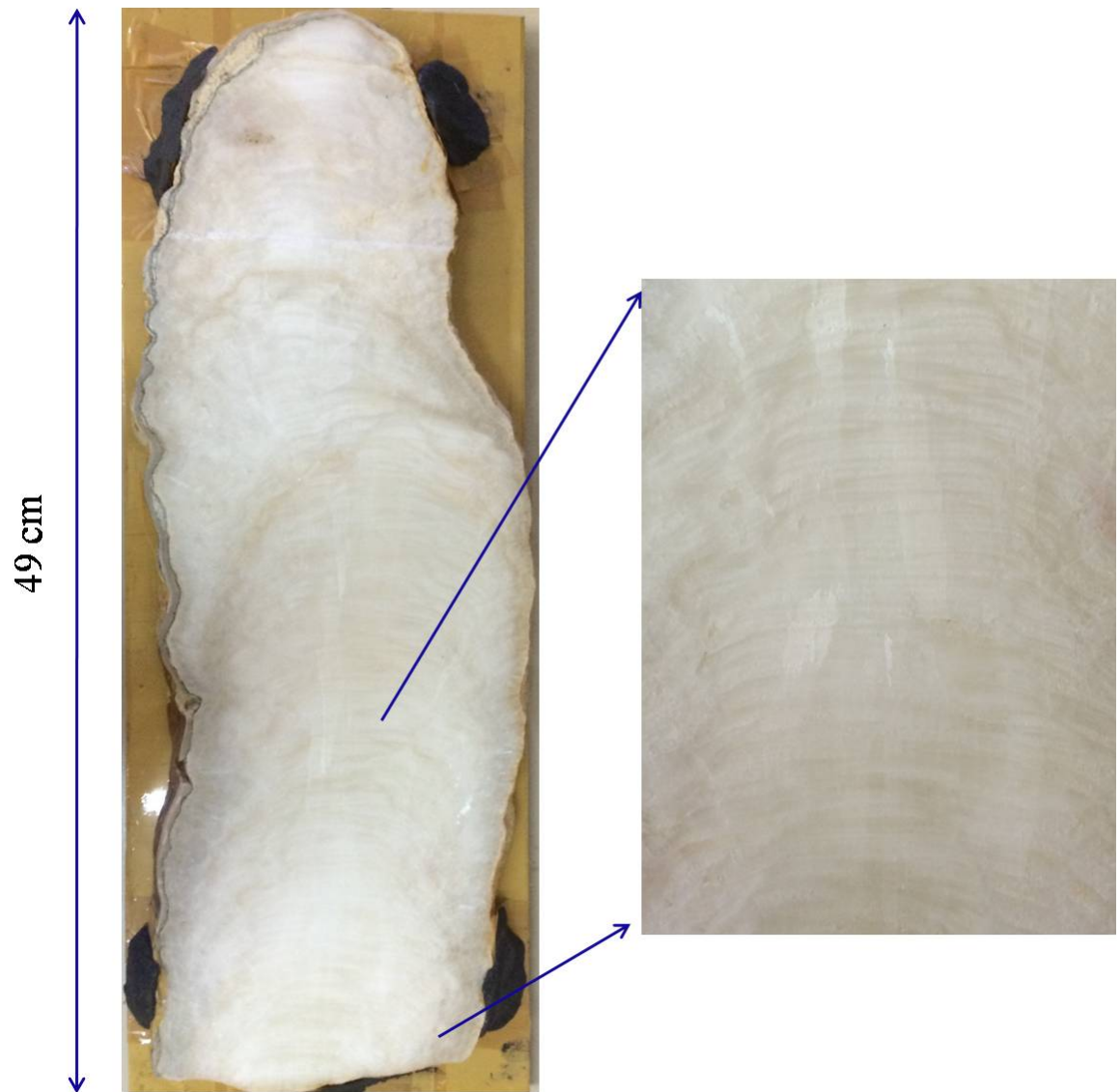


Figure 3.7: *Left: Photo shows the polished cross-section of Kailash stalagmite. The stalagmite growth is continuous and is made of calcite. The growth axis has shifted twice during deposition. Right: An enlarged view of the older section of the sample. Layers are visible to the naked eye and range from $\sim 1 - 2$ mm in thickness.*

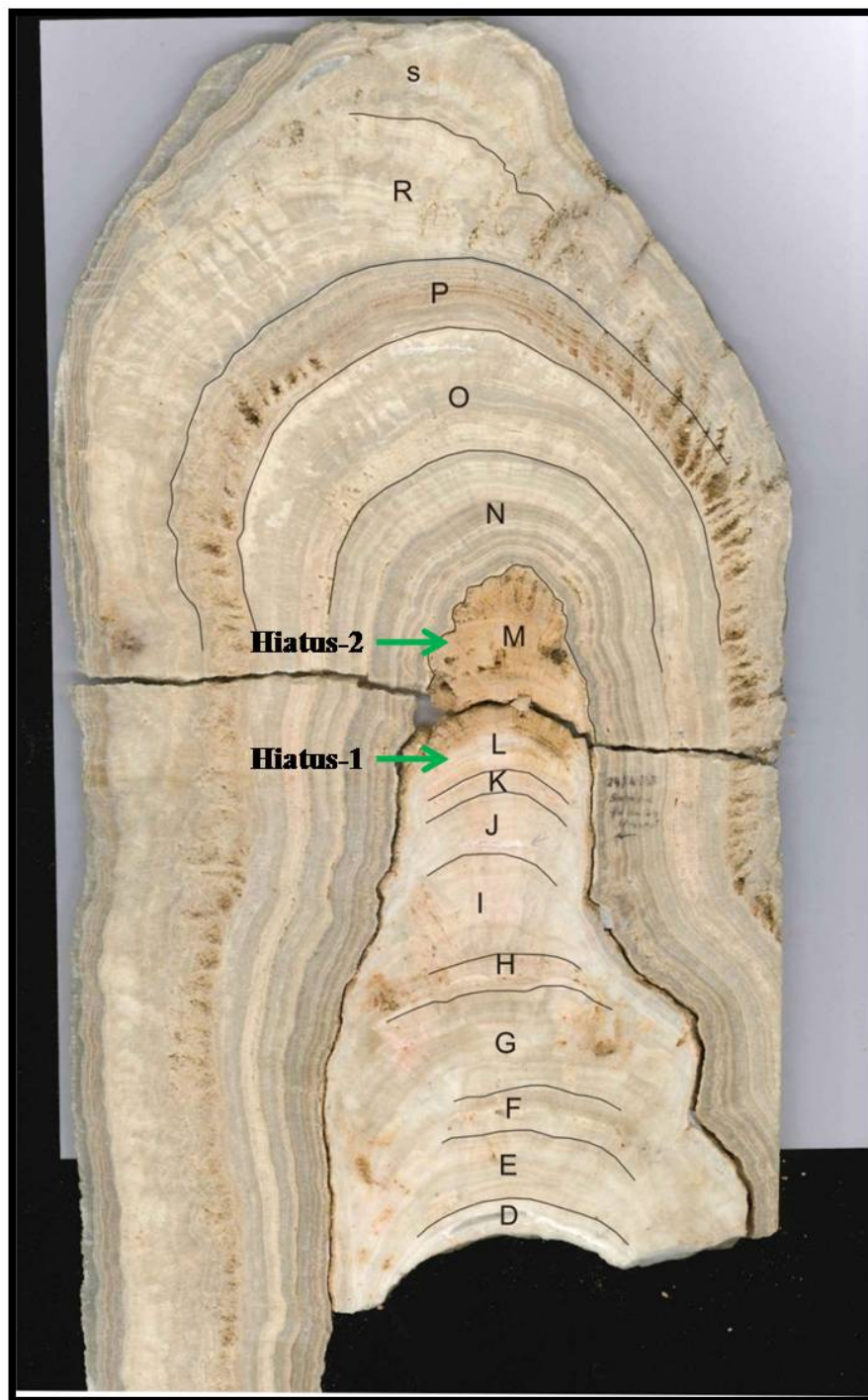


Figure 3.8: Photo shows the cross-section of the Belum stalagmite (BLM-1). The sample was divided into various bands based on the compositional changes, and for the ease of sampling. The green arrows show two distinct hiatuses, along the growth layers.

3.2 Stable Isotope and concentration measurements

3.2.1 Isotope ratio mass spectrometer (IRMS)

Analysis in the present study is by the use of two stable isotope mass spectrometers for isotopes of oxygen and carbon and a Q-ICP-MS (see below) for trace elements. The working principle of all the three mass-spectrometers is explained below.

Mass spectrometry is a technique of where ions are separated based on the mass to charge ratio. Mass spectrometer has three main components namely, the source, the analyzer and the detector (Figure 3.9). The roles of all the three parts are explained below.

1. **The source:** The source is the most diverse component of an instrument. In stable isotope mass spectrometry, electrons emitted from a filament are used to ionize the gaseous samples, whereas in an ICP-MS, the sample is injected in an aqueous medium and an argon plasma is used to ionize the sample.

The stable isotope mass spectrometer uses a thorium coated tungsten filament, to produce electrons (accelerated to ~ 70 eV energy) by passing ~ 3.5 A current through it. Upon entering the source, the gas (CO_2) gets ionized with the an efficiency of 0.1%. A low magnetic field is applied to increase the ionization efficiency, wherein the electron move in spiral motion along the magnetic field. The ion beam is focused using collimating plates and a high voltage (~ 2.5 kV) accelerates the positively ionized gas molecules into the analyzer (Figure 3.9).

The Quadrupole- Inductively coupled plasma mass spectrometer (Q-ICP-MS) has a radio frequency inductively coupled argon plasma as an ion source. The aqueous samples are introduced to a nebulizer which converts

them to small aerosol droplets. A spray chamber transfers these aerosol droplets to a plasma torch, which is at a temperature of 6000°C. Here the sample in gaseous form is stripped of an electron and the ionized gas enters the interface. As the plasma operates at air pressure while the quadrupole operates at a very low pressure, an interface between them is required to reduce the pressure. The sample ions in the interface are directed through cones and skimmer into the quadrupole.

A charged (q) molecule in an accelerating voltage (V) obtains a kinetic energy.

$$qV = \frac{1}{2}mv^2$$

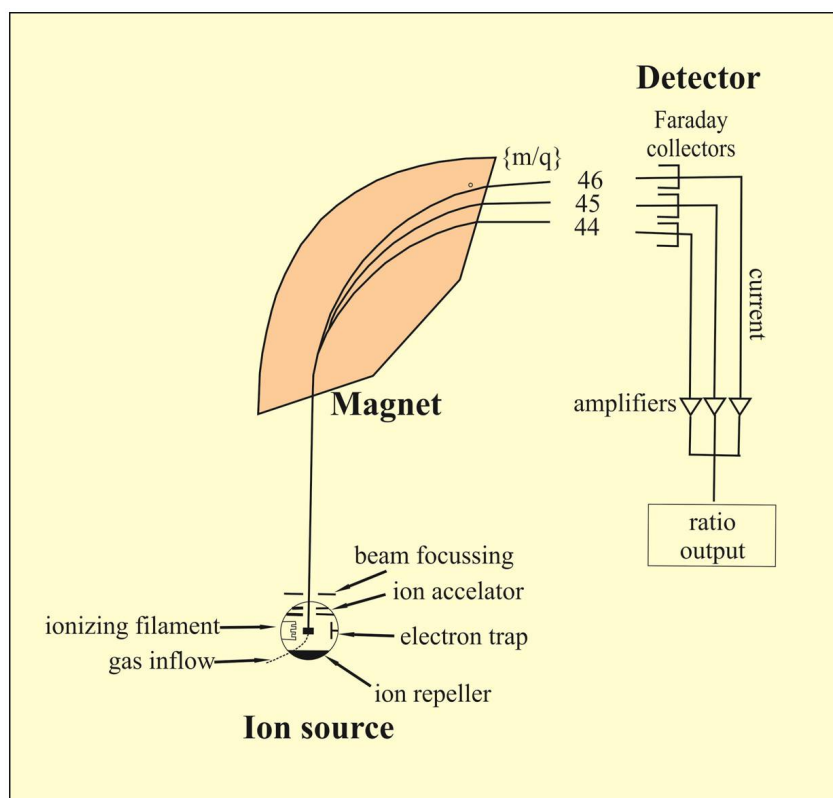


Figure 3.9: Sketch of a mass spectrometer with the three key components : source, analyzer and detector. Source: [Clark and Fritz \[1997\]](#)

2. **The analyzer:** For the analysis of carbon and oxygen isotopes of CO_2 prepared from the sample is introduced in the IRMS. A magnetic field of ~ 3.8 kG is applied perpendicular to the ion beam across the flight tube. The CO_2 ions are split based on the mass to charge ratio. In this case, three beams are produced. The motion of the ions is deflected and they follow curvilinear paths owing to the Lorentz force. This force imparts a centripetal acceleration to the ion beam entering perpendicular to the magnetic field.

$$q(\mathbf{v} \times \mathbf{B}) = \frac{mv^2}{r}$$

Hence the radius of curvature of the ion is,

$$r = \sqrt{\frac{2Vm}{\mathbf{B}^2 q}}$$

When V , B and q are constant, the radius of curvature of singly charged ion is directly proportional to the square root of its mass [Faure, 1977; Potts, 2012]. Hence, ions of heavier mass ($CO_2 = 46$) are deflected into a path of higher radius compared to the lighter ions ($CO_2 = 44$).

In Q-ICP-MS, the voltages and radio frequencies are managed so that at a given time, ions with a specific mass by charge ratio remain stable within the rods and pass through to the detector. The ions with different mass by charge ratio are rejected (Figure 3.10). To cover the mass range of interest, the electronics rapidly changes the quadrupole settings to allow different mass-to charge- ratios to pass through. The quadrupole has a capacity of scanning at a rate of 5000 atomic mass units (amu) per second [Elmer, 2001].

3. **The detector:** The currents due to ion beams are measured using Faraday cups, which are attached to very high resistances $\sim 10^9 \Omega$. In IRMS,

ions produce a voltage across the resistance, which is measured. This is proportional to the number of ions entering into the cup per unit time.

In Q-ICP-MS, the ions exiting the mass spectrometer, strike the surface of an detector (dynode), releasing an electron each time an ion strikes it. The series of dynodes generate a cascading stream of electrons until a measurable pulse is generated. The system counts the ions that hit the first dynode converting it to a signal.

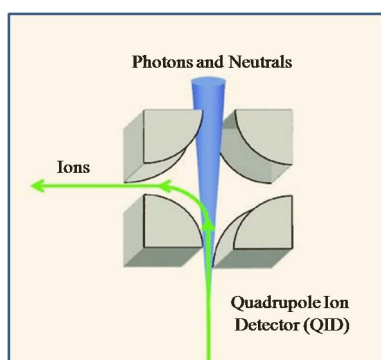


Figure 3.10: Schematic showing the working principle of quadrupole. The beam carries ions, photons, unionized particles and neutrals. The ions of selected mass pass through the detector, while photons and neutral particles are ejected out.



Figure 3.11: Photo shows Thermo Fisher Delta-V Plus IRMS on the left and Pal Gas-bench to the right at PRL.

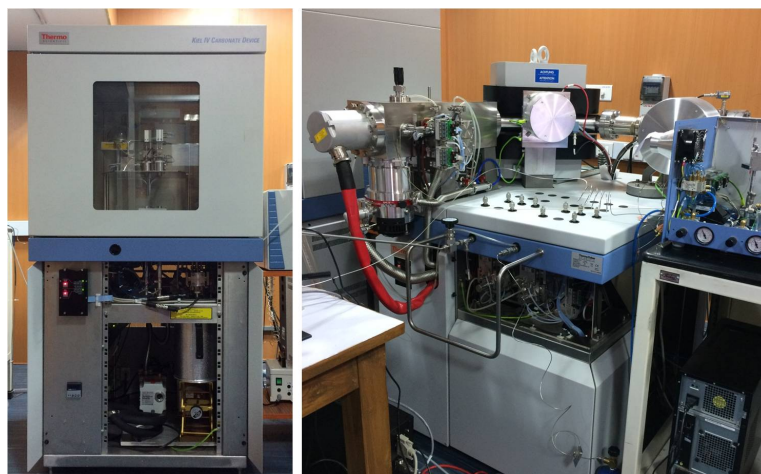


Figure 3.12: Photo shows Kiel-carbonate device to the left and Thermo Fisher MAT-253 IRMS to the right at PRL.

3.2.2 $\delta^{18}\text{O}$ and $\delta^{13}\text{C}$ measurements

Carbonate samples are converted to CO_2 by reacting the sample with 100% H_3PO_4 (Ortho-phosphoric acid), where the liberated CO_2 is directed to the mass spectrometer. Use of 100% H_3PO_4 is highly recommended as it is devoid of water and hence there is no variable contribution of oxygen isotopes from the water molecules. 100% H_3PO_4 acid is made by heating it at 120°C and slowly adding phosphorus pentoxide (P_2O_5), a dehydrating agent. The detailed procedure of preparing the acid is given by [Coplen et al. \[1983\]](#) and [Wachter and Hayes \[1985\]](#). Samples were measured on two mass spectrometers, namely, Delta V-plus IRMS (Figure 3.11) aided with Gas bench and MAT-253 aided with Kiel Carbonate device (Figure 3.12). The differences in components of both the IRMS are given in Table 3.1.

For the measurements in Delta v-plus, powdered carbonate samples were taken in 12 ml glass vials and tightly capped. The vials were then loaded onto the Gas Bench and flushed with He gas. Vials containing a laboratory carbonate standard, Makrana Marble (MMB), was placed in between the

Table 3.1: Sample preparation methods and mass spectrometric parameters used in the measurement of $\delta^{18}\text{O}$ and $\delta^{13}\text{C}$ in Delta V-plus and MAT-253 mass spectrometers.

	$\delta^{18}\text{O}/\delta^{13}\text{C}$	
	Delta V ⁺	MAT-253
Peripheral	Gas bench	Kiel carbonate device
Sample amount	500 μg	100 μg
Vial volume	12 ml	5.9 ml
Flushing gas	He (99.999 %)	He (99 %)/Ar
Flush time	12 minutes	-
CO_2 liberation time	1 hour	400 seconds
temperature	72°C	72°C
Electron energy	110 eV	110 eV
Faraday cups	5	10
High voltage	3 kV	10 kV
Separated ion beams	$^{12}\text{C}_{16}\text{O}_{16}\text{O}$ (44), $^{13}\text{C}_{16}\text{O}_{16}\text{O} + ^{12}\text{C}_{16}\text{O}_{17}\text{O}$ (45) $^{12}\text{C}_{16}\text{O}_{18}\text{O} + ^{13}\text{C}_{16}\text{O}_{17}\text{O} + ^{12}\text{C}_{17}\text{O}_{17}\text{O}$ (46)	
Correction	Craig correction	
Internal precision	0.06‰	0.04‰

sample vials at regular intervals. The needle used for flushing has two openings, one of the opening forces He gas into the vial, and the air within is flushed out through the other hole, which is then released out through the fused-silica capillary. After flushing, ~ 0.1 ml of ortho-phosphoric acid is injected manually using 1ml syringe. The samples are kept at 72°C for an hour to ensure complete the liberation of CO_2 gas. The CO_2 gas is then directed to the mass-spectrometer through the analysis needle. Figure 3.11 shows the photo of gas bench connected to Delta-V plus IRMS.

In the Kiel carbonate device, the sample powder is placed in vials and loaded onto a magazine(turret) with 44 slots. Ar/He is used as a carrier gas. The device has an automated acid injection system. After injecting the acid, the gas is carried through sample purification system comprising of two cold traps. The electronics attached to the traps ensures temperature changes from 0 to -190°C. The gas is trapped in liquid nitrogen at -190°C in the form of dry ice. At -80°C, pure CO_2 is liberated, whereas the moisture remains

in the traps. From the second trap, the purified CO_2 gas is transferred to the Dual inlet system of the mass spectrometer. The working principle of Kiel carbonate with MAT-253 IRMS is shown in Figure 3.13.

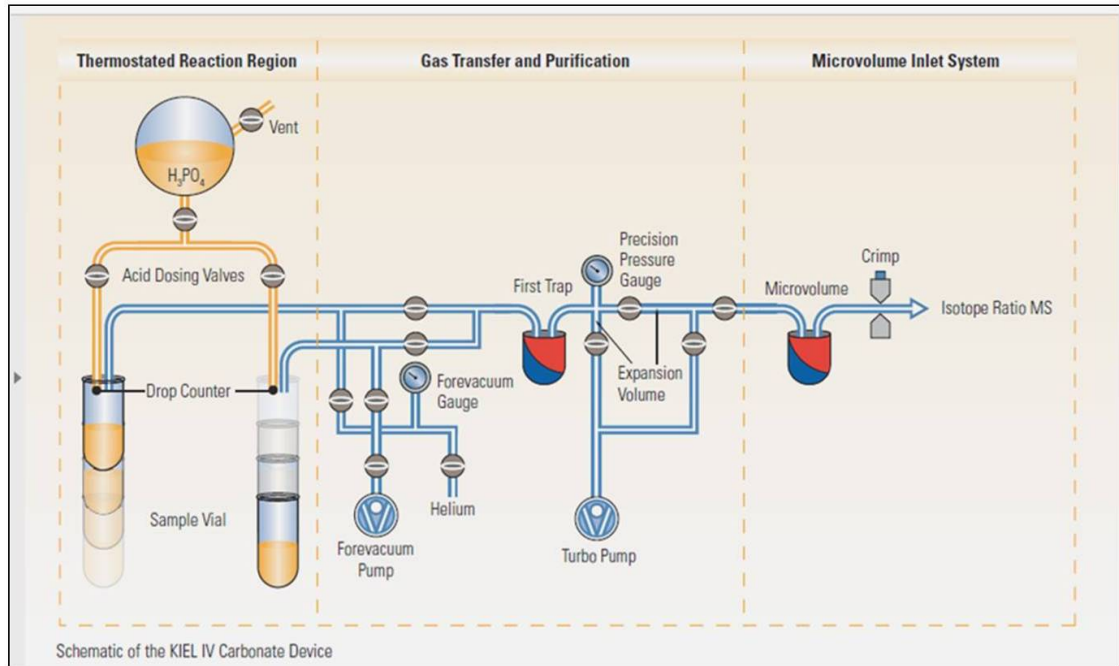


Figure 3.13: Working principle of Kiel carbonate connected to MAT-253 IRMS. Source: Instrument manual, Thermo Scientific

For the present measurements, continuous flow mode of Delta V-Plus and dual inlet mode of MAT-253 IRMS were used. In dual inlet there is alternation between a "reference" gas (of known isotopic composition) and a sample gas, whereas in the continuous flow, Helium is used as a carrier gas to carry sample to the source chamber. The details of sample preparation, equilibration and mass spectrometric conditions are listed in Table 3.1.

The sample isotopic abundances are reported with respect to VPDB (Vienna Pee Dee Belemnite) using the following conversion equation [Clark and

Fritz, 1997].

$$\delta^{18}O_{VPDB}^{Sample} = \delta^{18}O_{VPDB}^{MMB} + \delta^{18}O_{MMB}^{Sample} + (\delta^{18}O_{VPDB}^{MMB} \times \delta^{18}O_{MMB}^{Sample} \times 10^{-3}\text{‰}) \quad (3.1)$$

$$\delta^{13}C_{VPDB}^{Sample} = \delta^{13}C_{VPDB}^{MMB} + \delta^{13}C_{MMB}^{Sample} + (\delta^{13}C_{VPDB}^{MMB} \times \delta^{13}C_{MMB}^{Sample} \times 10^{-3}\text{‰}) \quad (3.2)$$

Here, MMB is the laboratory standard and stands for Makrana marble with 99.99% pure $CaCO_3$. MMB has been calibrated with respect to International standard (VPDB) and the values are:

$$\delta^{18}O_{VPDB}^{MMB} = -10.7\text{‰} \quad (3.3)$$

$$\delta^{13}C_{VPDB}^{MMB} = 3.9\text{‰} \quad (3.4)$$

Since the mass spectrometer measures the values of $\delta^{18}O_{ref}^{sample}$ and $\delta^{18}O_{ref}^{MMB}$ (ref=reference gas), the $\delta^{18}O_{MMB}^{Sample}$ is calculated from the following equation

$$\delta^{18}O_{MMB}^{Sample} = \delta^{18}O_{ref}^{sample} + \delta^{18}O_{MMB}^{ref} + (\delta^{18}O_{ref}^{sample} \times \delta^{18}O_{MMB}^{ref} \times 10^{-3}\text{‰}) \quad (3.5)$$

where $\delta^{18}O_{MMB}^{ref}$ is,

$$\delta^{18}O_{MMB}^{ref} = \frac{-\delta^{18}O_{ref}^{MMB}}{\left(\frac{\delta^{18}O_{ref}^{MMB}}{1000}\right) + 1} \quad (3.6)$$

Using equations(1.3,1.5 and 1.6) the values of $\delta^{18}O_{VPDB}^{Sample}$ are calculated. Similarly, calculations were done to derive $\delta^{13}C$ values of carbonate samples. The mass spectrometer measures ratios of 44/46 and 45/46 for $\delta^{18}O$ and $\delta^{13}C$ respectively. The corrections applied to remove isobaric interferences are explained below.

Craig correction: The masses 45 and 46 have small contribution from very low abundant isotopes of ^{13}C and ^{17}O . When these molecular ratios are converted into atomic ratios, a correction is required to eliminate the effect of $^{13}\text{C}^{16}\text{O}^{17}\text{O}$ from $^{12}\text{C}^{16}\text{O}^{18}\text{O}$ ($\delta^{18}\text{O}$), which is called Craig correction [*Craig, 1957*].

$$\delta^{13}\text{C} = 1.0676\delta_{45} - 0.0338\delta_{46}$$

$$\delta^{18}\text{O} = 1.0010\delta_{46} - 0.0021\delta_{45}$$

The accuracy and precision of the measurement were checked time to time using the international standards procured from IAEA. The reported isotopic values of the different standards procured from IAEA are given in Table 3.2. Of these standards, NBS-19 and IAEA-CO-1 were used for cross-checking the values of laboratory standard MMB. Table 3.3, shows the comparison between reported and measured values of IAEA standards. The measured values are averages of 20 analyses of each of the standards.

Table 3.2: IAEA standards used for carbonate and water isotope measurements.

IAEA primary standards				
Name	Nature		$\delta\text{‰}$	Reference standard
V-SMOW	water	$^2\text{H}/^1\text{H}$	0	V-SMOW
		$^{18}\text{O}/^{16}\text{O}$	0	V-SMOW
SLAP	water	$^2\text{H}/^1\text{H}$	-428.0	V-SMOW
		$^{18}\text{O}/^{16}\text{O}$	-55.50	V-SMOW
NBS-19	calcite	$^{13}\text{C}/^{12}\text{C}$	1.95	V-PDB
		$^{18}\text{O}/^{16}\text{O}$	-2.20	V-PDB
Intercomparison materials				
GISP	water	^2H	-189.73 ± 0.87	V-SMOW
		$^{18}\text{O}/^{16}\text{O}$	-24.784 ± 0.075	V-SMOW
NBS-18	calcite	^{13}C	-5.029 ± 0.049	V-PDB
		^{18}O	-23.035 ± 0.172	V-PDB
IAEA-CO-1	calcite	^{13}C	2.48 ± 0.025	V-PDB
		^{18}O	-2.437 ± 0.073	V-PDB
IAEA-CO-8	calcite	^{13}C	-5.749 ± 0.063	V-PDB
		^{18}O	-22.667 ± 0.187	V-PDB

Table 3.3: Comparison between reported (above) and measured (present work) values of IAEA standards

Delta-vplus/Mat-253				
Standard	$\delta^{18}\text{O}$ reported	$\delta^{18}\text{O}$ Measured	$\delta^{13}\text{C}$ reported	$\delta^{13}\text{C}$ reported
NBS-19	-2.20	-2.22 ± 0.08	1.95	2.1 ± 0.07
IAEA-CO-1	-2.44	-2.49 ± 0.03	2.48	2.42 ± 0.072

3.2.3 Trace element analysis

Trace element studies of the Belum and the Kailash stalagmites were carried out on a Q-ICP-MS at PRL (Figure 3.14). 100 subsamples from the Belum

stalagmite were milled using a dentist drill at the resolution of 3 mm for major and trace element analyses. Around 200 subsamples of Kailash stalagmite were prepared, each by clubbing 15 subsamples milled for stable isotope analysis. Each of subsamples weighed 6 to 10 mg. For trace element measurements the procedure described by [Eggins *et al.*, 1997] and modified by [Zhou *et al.*, 2008] was used. Samples were milled in a clean environment and ~ 6 mg was dissolved in 10 ml 2% nitric acid. The 10 ml solution with a dilution factor of 1666 is used as a stock solution. Sensitivity of the machine lies between 1 ppb to 1 ppt. Hence, major elements like Ca and Mg need significant factors of dilution. Two sets of dilutions were made; one for high weight percentages of Ca and the other for low concentrations of Mg, Sr and Mn. The aliquots used for Ca measurement was diluted 400 times and the aliquots prepared for trace element measurements were diluted only 4 times the volume. Since the solution had no residue, no further processing was required and they were measured directly on the Q-ICP-MS. For internal standardization, multiple enriched isotopes of ^{69}Ga – ^{115}In – ^{209}Bi were used. A synthetic limestone standard, JLS-1 was used for external calibration. The concentrations of elements of interest in the standard are shown in Table 3.4. External calibration is done using known dilutions of the standard and plotting a linear diagram of concentrations versus the counts. Once the calibration curve is ready, counts of a sample with unknown concentration can be mapped on the calibration curve and its respective concentration can be estimated. The calibration curves for the elements measured are shown in figure 3.15. The concentrations of Mg, Sr and Mn were normalized with that of Ca. Samples were altered with blank solutions to check the consistency of measurements. For cross-calibration of the measurements, JDo-1, an artificial Dolomite rock standard was run as an unknown.



Figure 3.14: *Thermo-scientific Quadrupole-Inductively Coupled Plasma mass spectrometer at PRL, Ahmedabad.*

Table 3.4: *International standards used for trace element measurements. * marks the major elements in % and minor and trace elements are reported in ppm.*

GSJ Geochemical Reference Standards

Element	JLs-1	JDo-1
Cao*	55.09	33.96
MgO*	0.606	18.47
MnO*	0.00209	0.00657
Sr	295	116
Ba	476	6.14
U	1.75	0.858
Th	0.0287	0.0429
Zn	3.19	35.4

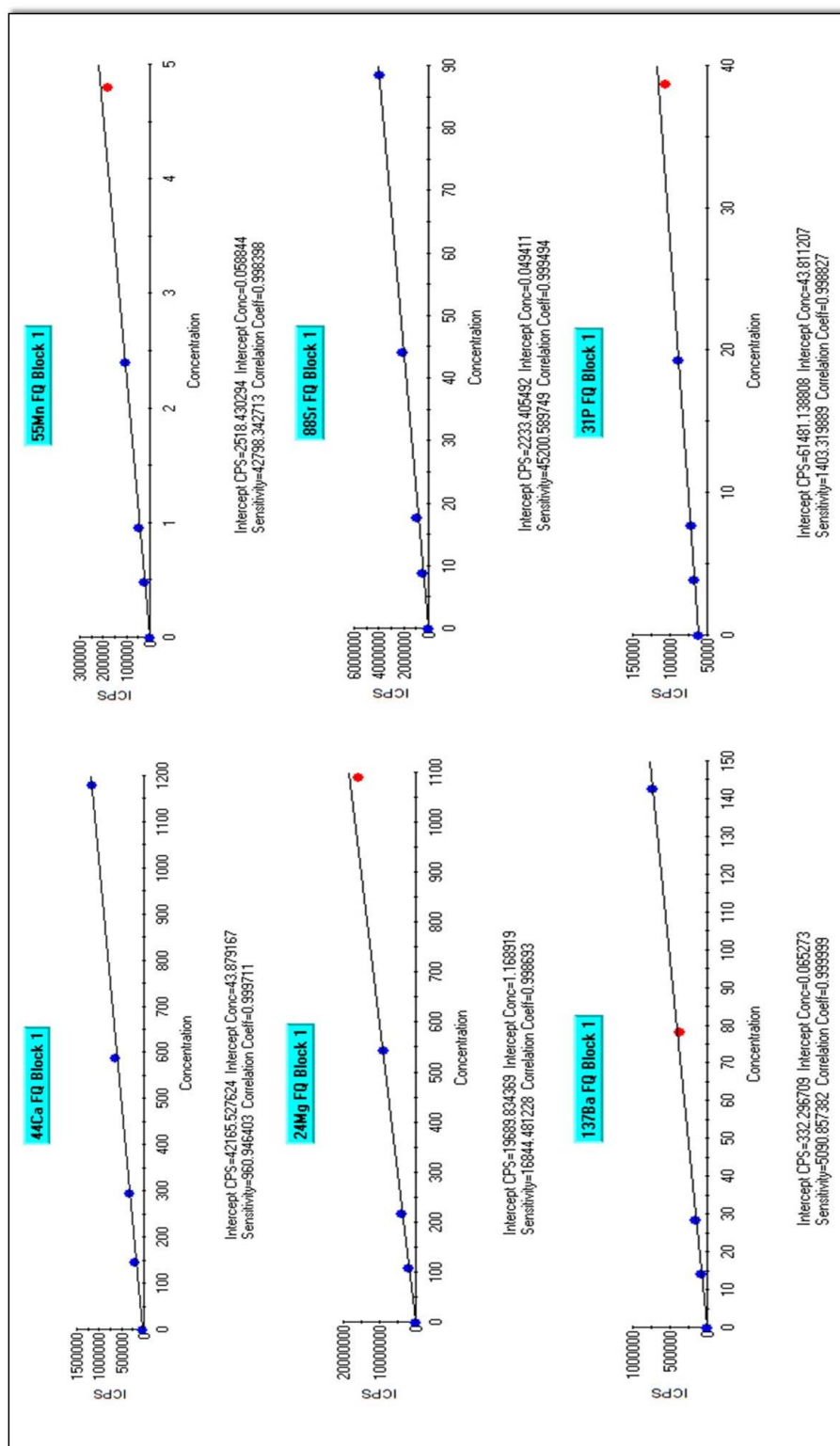


Figure 3.15: Typical calibration curves for different trace elements generated on ICP-MS using various dilutions of JLS-1.

3.3 Additional data used

To reconstruct monsoon from $\delta^{18}O$ of stalagmites, it is first essential to establish the existence of "amount effect" in the sampling region. The isotope values of rainwater samples for a long duration of time were taken from the Global Network of Isotopes in Precipitation (www.iaea.org).

3.3.1 Global Network of Isotopes in Precipitation (GNIP)

The IAEA's Water Resources Programme and the World Meteorological Organization (WMO) has established a global network for surveying the stable $\delta^{18}O$ and δD and tritium concentrations in the worldwide precipitation since 1961 CE. The data is archived at www.iaea.org/water/. In the present study, $\delta^{18}O$ and the corresponding rainfall amount over the study region is used from the GNIP data.

3.3.2 Reanalysis/satellite data

Wind field and specific humidity data were taken from the National center for Environmental Prediction reanalysis-1 [NCEP, [Kalnay et al. \[1996\]](#)]. And the monthly rainfall data were taken from Global Precipitation Climatological Project[GPCP, [Adler et al. \[2003\]](#)].

Along with the "amount effect", it is also important to know the source of precipitation over a region. This is verified using HYSPLIT models explained below.

3.3.3 Hybrid Single-Particle Lagrangian Integrated Trajectory (HYSPLIT)

HYSPLIT model is used to understand the trajectories of an air parcel reaching the sampling region. The model is forced using data from Global Data Assimilation System (GDAS). The advection of the air parcel is calculated from the position (grid point) and 3D wind field (V). At each time step, the model calculates a guess position and the velocity vectors are linearly interpolated in both space and time. The first guess position is

$$P'_{t+\Delta t} = P_t + V_{P,t}\Delta t$$

and the final position is,

$$P'_{t+\Delta t} = P_t + 0.5(V_{P,t} + V_{P',t+\Delta t})\Delta t$$

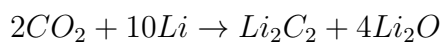
The integration time Δt varies from 1 hour to 1 minute depending upon the prevailing wind speed. The model also provides meteorological parameters such as temperature, potential temperature, relative humidity and height of the parcel above the mean sea level along the trajectory. In the present study back trajectory at 1500 m above ground level was calculated by the HYSPLIT.

3.4 Radiocarbon dating

Radiocarbon dating was used to assign ages to the KOT-I stalagmite. The sample was converted to benzene and liquid scintillation counter was used to measure the residual ^{14}C activity. The detailed procedure of benzene synthesis is explained below.

1. **Wet combustion** Four subsamples from the KOT-I stalagmite were extracted using dentist drill. Each subsample covering many growth laminae and weighing $\sim 5 - 8g$, were taken in round bottom flask connected to the vacuum line, pumped by a rotary pump. To ensure minimum loss of sediments, the powder was wetted with distilled water and evacuated. Dilute H_3PO_4 acid was added slowly to the flask and the solution was churned with magnetic stirrer to confirm complete liberation of CO_2 [Agrawal and Yadava, 1995; Gupta and Polach, 1985; Yadava and Ramesh, 1999]. The gas was then passed through two subsequent moisture traps maintained at $-80^\circ C$ using a slush(ethanol + liquid nitrogen) for water vapor trapping. The purified CO_2 was trapped in liquid nitrogen (LN_2) at $-190^\circ C$. With additional trapping and purification, CO_2 was then stored in glass flasks for acetylene preparation. The CO_2 extraction and purification glass line are shown in Figures 3.16 and 3.17 .

2. **Acetylene Preparation** In this step, CO_2 from the sample was converted to Acetylene. For this purpose, 6g of pure lithium metal is melted at $750^\circ C$ in an evacuated reaction chamber (Figure 3.18). 6 g of lithium is required for CO_2 equivalent to 1 g of carbon. At $550^\circ C$, CO_2 is passed to reaction chamber(Figure 3.16), where it reacts to form Lithium carbide (Li_2C_2). The reaction should be carried out very slowly to ensure no elemental carbon is formed. The reaction proceeds as follows:



After reaction the vessel is cooled to room temperature for hydrolysis.

3. **Hydrolysis** The process of hydrolysis involves reaction of distilled ground water with Lithium carbide. Ground water is used as there is no tritium activity and hence no interference is observed while counting. The reaction is exothermic, and hence should be carried out very slowly. The reaction proceeds as follows

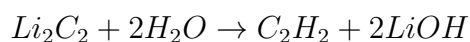


Figure 3.16: Photo shows the benzene synthesis glass line at PRL on the left and reaction chamber on the right.

The acetylene is removed by cryogenic pumping. It is passed through moisture trap at -80°C to remove traces of water vapor. As shown in the figure 3.18, the gas passes through the a trap filled with glass beads coated with NaOH and H_3PO_4 and subsequently through the trap filled with sodalime. They are used to remove the trace gases from the acetylene. The acetylene is collected using two traps, maintained at -190°C using liquid nitrogen. The gas is slowly passed to a column containing a catalyst, vanadium pentoxide (V_2O_5) pellets. The process is exothermic, and hence the column is cooled for a long time.

- 4. Benzene synthesis** The catalyst helps in polymerization of acetylene (C_2H_2) to Benzene (C_6H_6). Benzene is recovered from the column by heating it to 110°C [Polach et al., 1972] and trapping it in a vial at -190°C using

liquid nitrogen. The catalyst is reactivated at about 300°C by periodically passing dry air (through molecular sieve) into the column. The overall chemical yield is between 90-94% [Yadava, 2002].

Conversion to benzene is important for two reasons. The first reason is that benzene is a molecule with very small atomic structure containing the maximum number of carbon atoms. And the second is that the benzene solution has high transmission and low absorption for scintillation. As a result very little counts are lost.

The benzene thus obtained was made up to 1 ml and an organic scintillator (Butyl-PBD, 0.015 g per ml) is added to it for converting the β particle to photons and assayed to a low background Liquid Scintillation Counter (LSC) in a teflon vial.

The schematic of benzene synthesis line is shown in figure 3.18.

To estimate the background activity, an anthracite sample with no radiocarbon activity is used. The modern reference activity is periodically calculated from Oxalic acid-I and Oxalic acid-II provided by the U.S. National Bureau of Standards by converting them to benzene. As these compounds are organic in nature, CO_2 is produced from them using dry combustion. The samples were heated in a quartz tube to produce carbon dioxide under continuous flow of oxygen. Carbon monoxide present in trace amounts was removed by oxidizing it using CuO mesh heated at 550°C. The carbon dioxide was purified by passing it through the chemical traps filled with the solutions of KI/I_2 , $AgNO_3$ and $H_2SO_4/K_2Cr_2O_7$. The procedure for acetylene and Benzene preparation follows the same protocol as described above.

Liquid Scintillation counter(LKB-QUANTULUS) ^{14}C decays by the emission of β^- particles. The energy levels of these particles range from 0 to 156 keV.

These particles have kinetic energy which is transferred to the solvent molecules of the scintillator. These excited solvent molecules then transfer their energy to the scintillator molecules. A stable energy state leads to emission of photons proportional to energy of the emitted particle. Scintillation solutions comprise of primary and secondary scintillators. Primary scintillator is a solution which converts excitation energy into photons. The important function of the secondary scintillators is to shift the wavelengths of the photons emitted from 370 nm to 420 nm. Thus they act as wavelength shifters. The most widely used secondary scintillator is POPOP [1,4 – bis-(2-(5-Phenyl-oxazolyl))-benzene].

In order to detect the photons efficiently photosensitive device is used. Scintillation counter has two photo multiplier tubes (PMTs) which collect the total light produced in the scintillation vial and convert the absorbed photon energy into electrical energy by the release of photoelectrons. Thus the PMT amplifies the signal such that the amplitude of the pulse is directly proportional to the number of photons detected by the photo cathode. The counting period is set to 85 minutes duration and 30 repeat runs are done for statistically sound results. The average background for 1ml of benzene 0.30 ± 0.03 cpm and the modern reference is 9.36 ± 0.13 cpm per ml of benzene measured (over a period of a year) with an overall precision of 1.5% Modern [Yadava, 2002]. The laboratory dating limit is 40 kyr [Yadava, 2002]. The isotopic fractionation associated with CO_2 to C_6H_6 conversion is minimal; depletion of $1.7 \pm 1\%$ is observed [Panarello et al., 1983; Yadava, 2002]. These values correspond to age overestimation by only 10-45 years. Radiocarbon age (T) equation is given as:

$$T = (1/\lambda).ln(A_{abs}/A) \quad (3.7)$$

A = net activity of the sample

A_{abs} = original equilibrium ^{14}C activity of the reservoir that supplied the sample.

This is obtained using reference materials e.g. oxalic-I and oxalic-II.

$\lambda = 1.21 \times 10^{-4} \text{yr}^{-1}$ is the ^{14}C decay constant (half-life of 5730 years)

The results of the Kotumsar caves are discussed in chapter 4. In the case of speleothems, a discrepancy exists as there are two sources of carbon to the precipitating calcite; modern CO_2 and the carbon from limestone rock (dead carbon). The contribution from each of these sources may vary and the resultant calcite may overestimate the age if it has excess carbon from the limestone. Hence, recourse is taken to the more precise ^{230}Th dating technique.

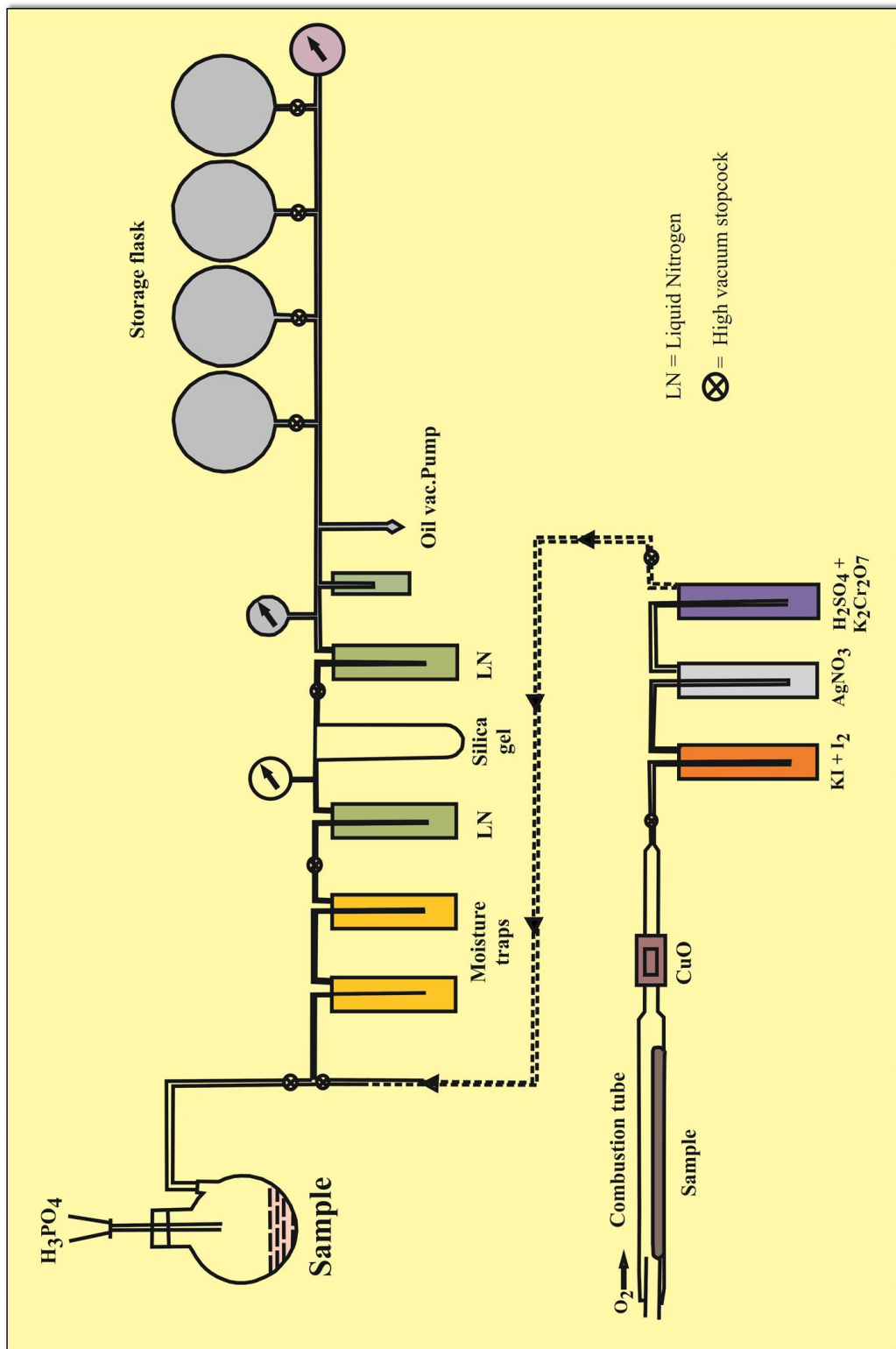


Figure 3.17: Schematic representation showing Wet and dry combustion setup for radiocarbon dating.

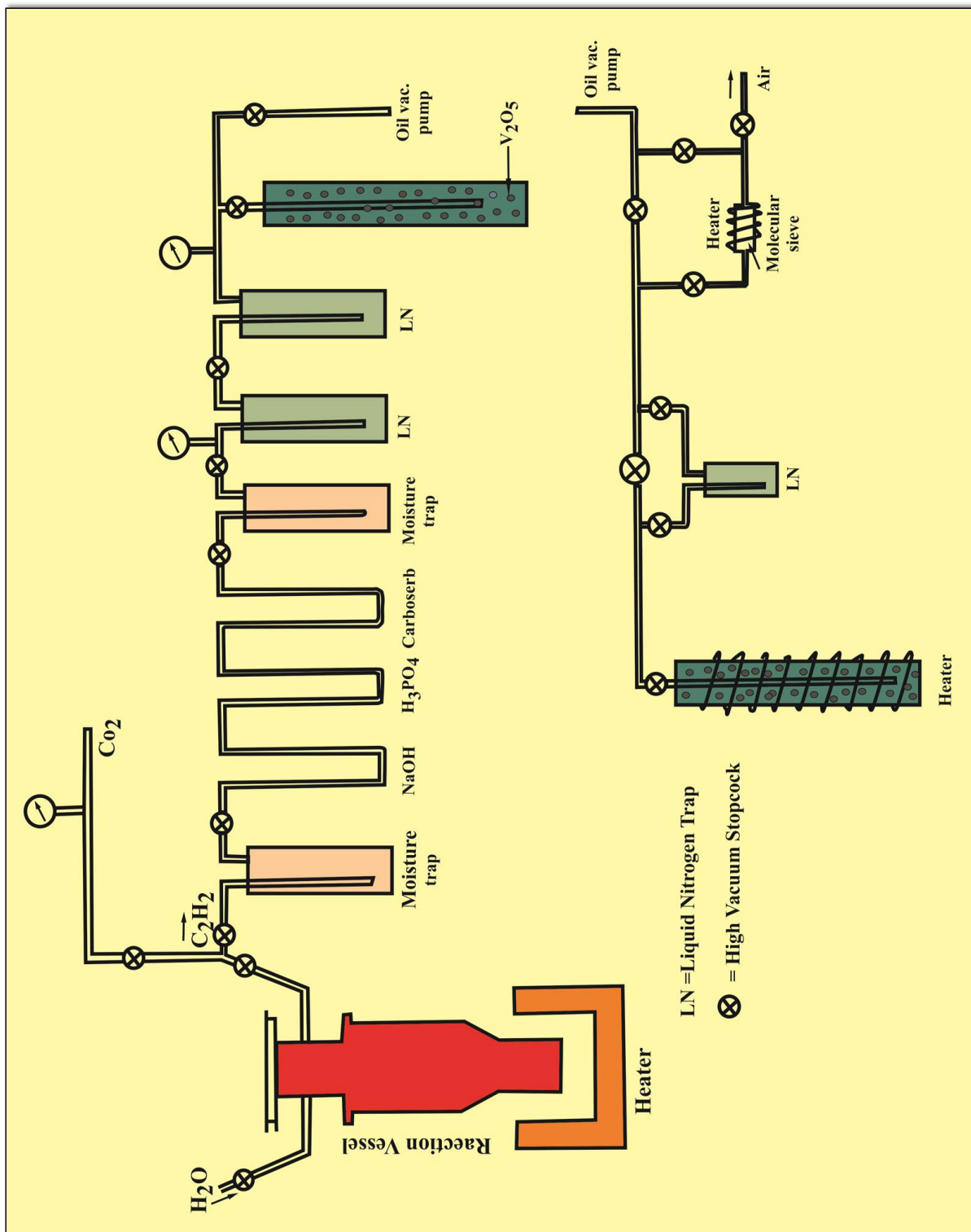


Figure 3.18: Schematic diagram showing acetylene and benzene synthesis setup.

3.5 U-Th dating

All the samples including KOT-I, were dated using the uranium-thorium dating technique. An overview of the systematics is given below.

3.5.1 Principles of dating

U-Th dating systematics is used on carbonates with accretionary growth (corals and speleothems) and deposited as a closed system. Precise age estimation can span from hundreds to over 500,000 years [*Edwards et al.*, 1987; *Henderson*, 2006; *Scholz and Hoffmann*, 2008]. The technique does not rely upon the long decay series of ^{238}U to ^{206}Pb , instead it is based on the decay of its daughter product ^{234}U to ^{230}Th . U-Pb systematics under a closed system assumptions are in secular equilibrium, as the half-life of the parent nuclide is much greater than the intermediate daughter nuclide [*Faure*, 1977]. The secondary carbonate formed from dissolution and subsequent-precipitation, such as speleothems, however, is in disequilibrium due to incorporation of excess daughter nuclide or its deficiency as a result of nuclear or physical fractionation. Time required for the system to attain secular equilibrium is used to determine the ages of the sample.

The average continental abundance of U and Th are 1.7 and 8.5 $\mu\text{g g}^{-1}$ respectively [*Richards and Dorale*, 2003; *Wedepohl*, 1995]. However, their abundances in the aquatic system vary significantly, because of the different solubility indices of U and Th. Uranium mobilizes quickly in contact with water and gets oxidized from +4 to +6 oxidation state and forms Uranyl ion (UO_2^{2+}) and its complexes as seen in figure 3.19 [*Faure*, 1977]. Uranyl ion co-precipitates with carbonates to form a complex ($\text{UO}_2(\text{CO}_3)^{-3}$) and gets incorporated into the system. Whereas, Th remains in the reduced +4 state and instead adsorbs or precipitates on the sediments. Hence, the speleothems precipitating under clean environments are devoid of initial Th activity.

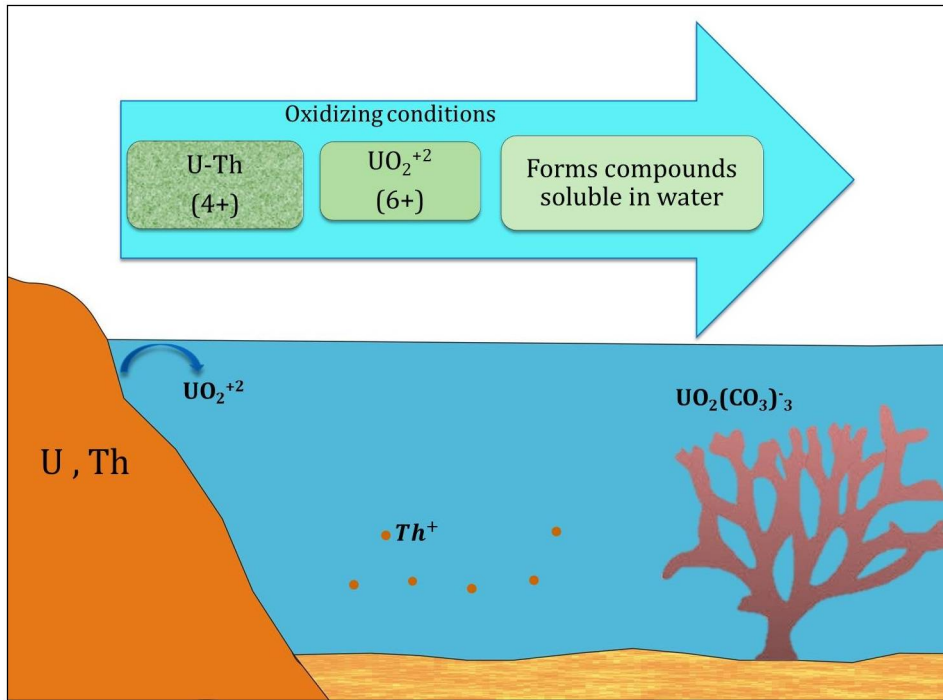


Figure 3.19: The schematic diagram explaining oxidation of uranium ion to form uranyl ion. Thorium adsorbs on the sediments and settles in water.

Hence, the $^{234}\text{U}/^{238}\text{U}$ activity is used to calculate the age of a speleothem, provided it's initial ratio while getting incorporated is known and the sample remained as a closed system. The final age equation, originally from Broecker (1963), was re-expressed by Haase-Schramm et al. (2004) as:

$$\left[\frac{^{230}\text{Th}}{^{238}\text{U}} \right] = (1 - e^{-\lambda_{230}t}) + \left(\left[\frac{^{234}\text{U}}{^{238}\text{U}} \right] - 1 \right) \times \left(\frac{\lambda_{230}}{\lambda_{230} - \lambda_{234}} \right) \times (e^{-\lambda_{234}t} - e^{-\lambda_{230}t}) \quad (3.8)$$

where, the square brackets imply the activity ratios, λ stands for decay constant and $t = \text{age}$. As the equation is transcendental, the age can be found out iteratively or graphically. The sample may have initial Th content adhering to the detrital particles, which is accounted by its measuring ^{232}Th activity. Higher ^{232}Th concentration implies higher amount of ^{230}Th . Corrections are made for the detrital ^{230}Th based on ^{232}Th concentration, used as a measure of contami-

nation and assuming appropriate $^{230}\text{Th}/^{232}\text{Th}$ ratio [Richards and Dorale, 2003]. The another approach to deduce the initial activities of Th and ^{234}U is to employ isochron technique. Isochrons can be plotted in two steps as given by Ludwig [2003].

1. $^{230}\text{Th}/^{232}\text{Th} - ^{238}\text{U}/^{232}\text{Th}$ and $^{234}\text{U}/^{232}\text{Th} - ^{238}\text{U}/^{232}\text{Th}$ referred as Rosholt type-II diagrams. The slope of the plots give the initial ^{230}Th and ^{234}U activities (Figure 3.20).
2. $^{230}\text{Th}/^{238}\text{U} - ^{232}\text{Th}/^{238}\text{U}$ and $^{234}\text{U}/^{238}\text{U} - ^{232}\text{Th}/^{238}\text{U}$ referred as Osmond type-II diagrams. The intercept of the plots give the initial ^{230}Th and ^{234}U activities (Figure 3.20).

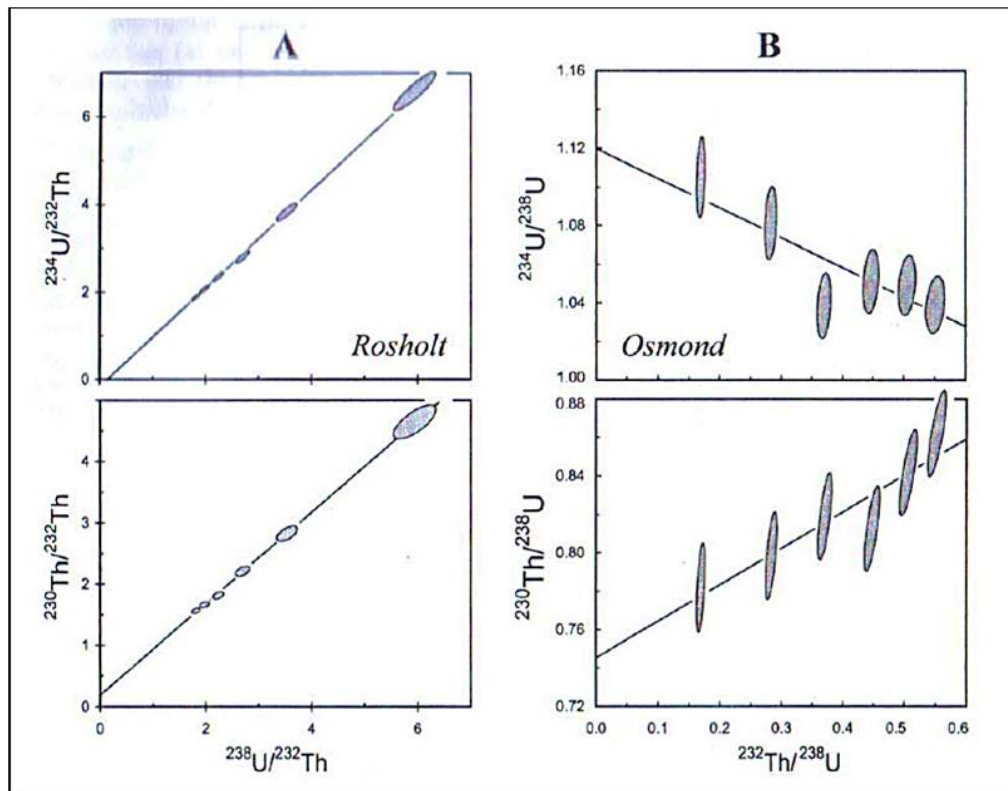


Figure 3.20: Rosholt and Osmond type plots used to determine for initial activities of ^{230}Th and ^{234}U in the sample [Ludwig, 2003].

3.5.2 Preliminary procedures

Since U-Th dating technique is crucial for speleothem based paleoclimate studies, an attempt was made to setup the technique at PRL. Much of the work is still under progress and the preliminary steps are discussed in brief.

Pre-concentration process Bulk carbonate sample consists of various trace elements, hence preferential removal of U and Th with maximum yield is important. Since the sample has trace amounts of U-Th, aerial contamination during extraction should be minimized. Hence, the pre-concentration procedures are carried out in a clean lab with class 1000 Hepa filters. U-Th separation from the matrix can be done using two types of Resins, namely, ion-exchange resin and chelating resin (UTEVA). In our work, we have used UTEVA resin, for removal of U and Th [Carter *et al.*, 1999; Horwitz *et al.*, 1992]. The maximum concentration of Uranium in speleothems can go up to is $170 \mu\text{g g}^{-1}$. For this reason, optimum carbonate sample quantity is 200 mg.

Resins are made of three main components: (a) the inner support, which is porous silica or organic polymer with size range of 50-150 μm (b) a stationary phase, which is liquid extractant and (c) a mobile phase, an acid solution. By changing the strength of the acids, different elements are leached out. In UTEVA (Uranium tetravalent Actinide) resin, the extractant is diamyl, amyl-phosphate (DAAP), which forms nitrate complexes with the actinide elements, which includes uranium and thorium. The formation of these complexes is driven by the concentration of nitrate in the sample solution. Therefore, at a higher strength of the acid (3M HNO_3) U(VI) and Th(IV) are retained by the resin, and the matrix elements(alkali earth) are separated out. In the next step, U-Th elution from the actinides is provoked by changing 3M HNO_3 to 3M HCl or changing the strength of 3N HNO_3 to 0.01M HNO_3 [Horwitz *et al.*, 1992]. In such conditions, the retention coefficient of thorium in HCl is less than that of uranium, favoring a good separation between the two elements. The protocol will be re-

fined by the measuring the concentration of elements collected in each elute and thereby changing the acid strength till the maximum recovery of U-Th. ^{229}Th and ^{236}U double spikes will be used to correct for the instrument introduced mass fractionation [Rudge *et al.*, 2009]. The final aliquots will be measured on a multi-collector-ICP-MS, using the procedures given by [Seth *et al.*, 2003; Shen *et al.*, 2002].

Age model After obtaining the U-Th ages, it is important to construct a reliable age model. Previously, most scientists opted for a linear interpolation between two-subsample distances. At present, speleologists use various age models like StalAge, COPRA, OXCAL, to name a few [Scholz *et al.*, 2012]. Each model comes with its own advantages and drawbacks. Our work is based on using the free software package COPRA 1.0, which is an interactive software that runs on the MATLAB interface [Breitenbach *et al.*, 2012]. Prerequisites to using this model is monotonicity i.e. the older deposition is at the bottom and younger at the top. Based on the ages and errors associated with them, a normal distribution is built around the age and proxy data points. The software uses 2000 Monte-Carlo simulations to interpolate between two data points. Age reversals and outliers can be identified and removed from the data set. The model also incorporates and interpolates ages between the hiatuses. The median of the distribution and the 95% confidence limits represent the final age model. The schematic of typical age model derived from COPRA is shown in figure 3.21.

For the speleothems reported in this study, the U-Th ages were obtained from the Oxford University, the University of New Mexico and the National Taiwan University. The results will be discussed in chapter 4.

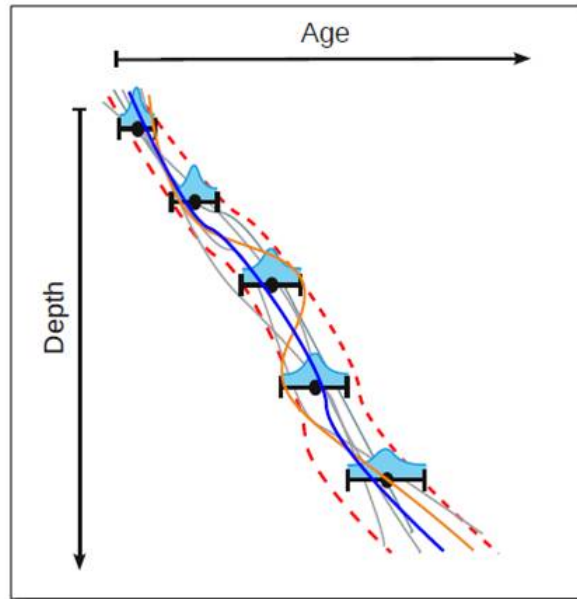


Figure 3.21: Schematic of the Monte Carlo model. The data points are plotted with the normal distribution (Cyan shaded area). The Standard deviation is equal to measurement error. The gray and brown curves indicate several realizations of the Monte Carlo simulation. The median blue curve and the 95% confidence limits (red dashed curves) represent the final age model resulting from the distribution of 2000 simulations. The image is taken from Breitenbach et al. [2012].

3.6 Foraminifera stable isotope analysis

The 4 m sediment core raised from the Andaman sea was composed of gray to very dark gray silty clay and seven discrete layers of tephra. After retrieval, it was divided into two parts, one for dating and stable isotope measurements and the other for geochemical and radiogenic isotope studies [Awasthi et al., 2014]. Planktic foraminifera were separated from the sediment core at intervals of 2 cm. The top 2 m of the core was dated using Accelerator Mass Spectrometer (AMS) radiocarbon dating of mixed planktic foraminiferal samples (collected from 10 different depths) at the AMS laboratory of University of Arizona, USA. The dates were converted into calendar ages using Marine-09 calibration curve [Reimer et al., 2009] and Calib 6.0 [Stuiver and Reimer, 1993]. A reservoir age

correction of ΔR (i.e., the difference between the regional marine ^{14}C age and the global model marine ^{14}C age) = $11 \pm 35(1\sigma)$ yr was assumed for the Andaman Sea [Awasthi *et al.*, 2014; Dutta *et al.*, 2001]. The bottom 2 m of the core was dated based on five sediment samples using ^{230}Th -excess dating at PRL. Samples collected at 2 cm interval were sent to Delhi university for identification and separation of foraminiferal species. The $\delta^{18}O$ composition of *Globigerinoides ruber* (white) was measured on Delta V-Plus IRMS and the values are reported with respect to VPDB.